

Small-molecule activation of procaspase-3 to caspase-3 as a personalized anticancer strategy

Karson S Putt¹, Grace W Chen², Jennifer M Pearson², Joseph S Sandhorst², Martin S Hoagland³, Jung-Taek Kwon⁴, Soon-Kyung Hwang⁴, Hua Jin⁴, Mona I Churchwell⁵, Myung-Haing Cho⁴, Daniel R Doerge⁵, William G Helferich³ & Paul J Hergenrother^{1,2}

Mutation and aberrant expression of apoptotic proteins are hallmarks of cancer. These changes prevent proapoptotic signals from being transmitted to executioner caspases, thereby averting apoptotic death and allowing cellular proliferation. Caspase-3 is the key executioner caspase, and it exists as an inactive zymogen that is activated by upstream signals. Notably, concentrations of procaspase-3 in certain cancerous cells are significantly higher than those in noncancerous controls. Here we report the identification of a small molecule (PAC-1) that directly activates procaspase-3 to caspase-3 *in vitro* and induces apoptosis in cancerous cells isolated from primary colon tumors in a manner directly proportional to the concentration of procaspase-3 inside these cells. We found that PAC-1 retarded the growth of tumors in three different mouse models of cancer, including two models in which PAC-1 was administered orally. PAC-1 is the first small molecule known to directly activate procaspase-3 to caspase-3, a transformation that allows induction of apoptosis even in cells that have defective apoptotic machinery. The direct activation of executioner caspases is an anticancer strategy that may prove beneficial in treating the many cancers in which procaspase-3 concentrations are elevated.

A hallmark of cancer is its resistance to natural apoptotic signals¹. Depending on the cancer type, this resistance is typically a result of either up- or downregulation of key proteins in the apoptotic cascade, or of mutations in genes encoding these proteins². Such changes occur in both the intrinsic apoptotic pathway, which funnels through the mitochondria and caspase-9, and the extrinsic apoptotic pathway, which involves the action of death receptors and caspase-8. For example, mutations or alterations in proper concentrations of the proteins p53 (ref. 3), Bim⁴, Bax⁴, Apaf-1 (ref. 5), FLIP⁶ and many others⁷ have been observed in cancers and lead to a defective apoptotic cascade—one in which the upstream proapoptotic signal is not properly transmitted to activate the executioner caspases. As most apoptotic pathways ultimately involve the activation of procaspase-3, these genetic abnormalities are effectively ‘breaks’ in the apoptotic circuitry, and cells having these abnormalities proliferate uncontrolled.

Given the potential use of proapoptotic compounds for treating cancer, efforts have been made to develop therapeutics that target specific proteins in the apoptotic cascade^{8,9}. For instance, peptides or small molecules that bind p53 (ref. 10), proteins in the Bcl-2 family^{11–13} or the inhibitor of apoptosis proteins (IAPs)¹⁴ have proapoptotic activity, as do compounds that promote the oligomerization of Apaf-1 (refs. 15,16). However, because many of these compounds target early or intermediate positions in the apoptotic cascade, cancers with mutations in downstream proteins are likely to be resistant to their

effects. For therapeutic purposes it would be ideal to identify a small molecule that directly activates a proapoptotic protein far downstream in the cascade. Such a therapeutic strategy would have a higher likelihood of success if concentrations of that proapoptotic protein were elevated in cancer cells.

The conversion of procaspase-3 to caspase-3 results in the generation of the active ‘executioner’ caspase that subsequently catalyzes the hydrolysis of many protein substrates. Active caspase-3 is a homodimer of heterodimers and is produced by proteolysis of procaspase-3 (ref. 17). *In vivo*, this proteolytic activation typically occurs through the action of caspase-8 or caspase-9. To ensure that this zymogen is not prematurely activated, procaspase-3 has a tripartite acid ‘safety catch’ that blocks access to the Ile-Glu-Thr-Asp (IETD) site of proteolysis¹⁸. This safety catch enables procaspase-3 to resist autocatalytic activation and proteolysis by caspase-9 (ref. 18). The position of the safety catch is sensitive to pH; upon cellular acidification (as occurs during apoptosis) the safety catch is thought to allow access to the site of proteolysis, and active caspase-3 can be produced either through the action of caspase-9 or through an autoactivation mechanism¹⁸.

Cells from certain types of cancerous tissue have elevated concentrations of procaspase-3. A study of primary isolates from 20 individuals with colon cancer showed that on average procaspase-3 is elevated six-fold in such isolates relative to adjacent noncancerous tissue¹⁸. In addition, procaspase-3 concentrations are elevated in

¹Department of Biochemistry, ²Department of Chemistry and ³Department of Food Science and Human Nutrition, University of Illinois, Urbana, Illinois 61801, USA. ⁴Laboratory of Toxicology, College of Veterinary Medicine and Nano Systems Institute-National Core Research Center (NSI-NCRC), Seoul National University, Seoul 151-742, South Korea. ⁵US Food and Drug Administration, National Center for Toxicological Research, Jefferson, Arkansas 72029, USA. Correspondence should be addressed to P.J.H. (hergenro@uiuc.edu).

Received 19 June; accepted 27 July; published online 27 August 2006; doi:10.1038/nchembio814

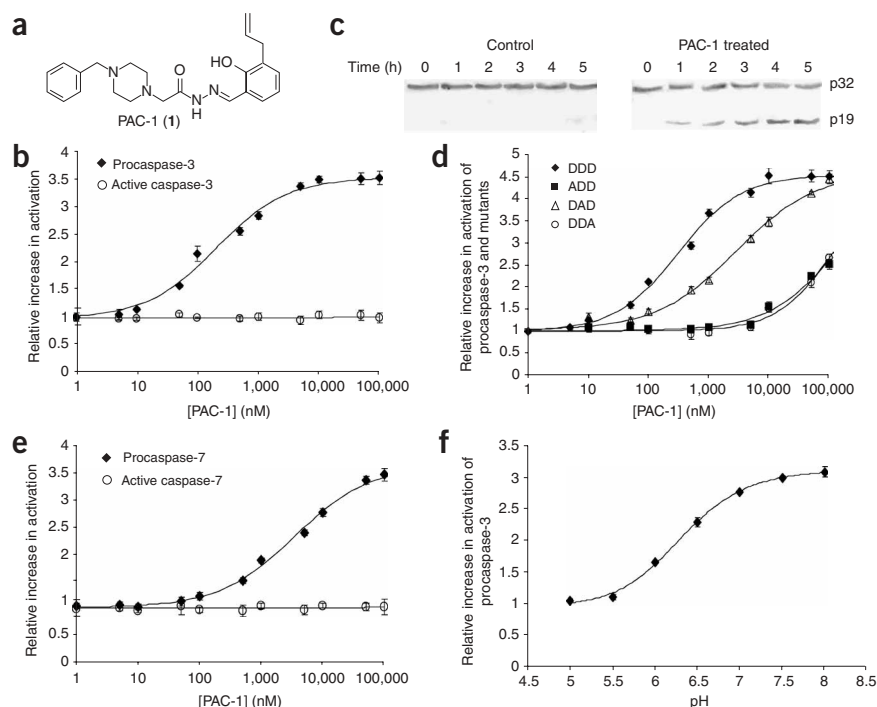


Figure 1 PAC-1 activates procaspase-3 *in vitro*. **(a)** Structure of PAC-1. **(b)** *In vitro* activation of procaspase-3 and active caspase-3 by PAC-1. PAC-1 activates procaspase-3 with an EC_{50} of 0.22 μ M. **(c)** Cleavage of procaspase-3 to active caspase-3 as induced by PAC-1. In this blot, the p32 band is the full-length, unprocessed procaspase-3, and the p19 band is the p17 fragment plus the prodomain and His6 tag. Procaspase-3 was recombinantly expressed in *E. coli* with an N-terminal His6 tag and purified. Immunoblotting was performed with an antibody to His6. In the absence of PAC-1 no maturation of procaspase-3 is observed. In the presence of 100 μ M PAC-1, cleavage to generate the mature large subunit (p19 fragment) is observed within 1 h, and >50% cleavage is observed after 4 h. PAC-1 is also effective at 5 μ M in this assay (**Supplementary Fig. 1**). **(d)** Activation of mutants in the safety-catch region of procaspase-3 by PAC-1. PAC-1 has an EC_{50} for activation of 0.22 μ M on wild-type procaspase-3 (DDD), and corresponding EC_{50} values of 2.77 μ M (DAD), 113 μ M (DDA) and 131 μ M (ADD) for the mutants. **(e)** PAC-1 activates procaspase-7 with an EC_{50} of 4.5 μ M. **(f)** Dependence of PAC-1 activation of procaspase-3 on pH. At low pH the safety catch is off and procaspase-3 is essentially maximally activated. Error bars are s.d.

certain neuroblastomas¹⁹, lymphomas²⁰, leukemias²¹, melanomas²² and liver cancers²³. In fact, a systematic evaluation of procaspase-3 concentrations in the panel of 60 cell lines used by the National Cancer Institute revealed that particular lung, melanoma, renal and breast cancers show greatly enhanced concentrations of procaspase-3 (ref. 24). Given the central importance of active caspase-3 to successful apoptosis, the high concentrations of procaspase-3 in certain cancerous cell types, and the safety catch-mediated suppression of its autoactivation, we reasoned that small molecules that directly activate procaspase-3 could be identified and that such molecules could have great potential in targeted cancer therapy. In this manuscript we report the *in vitro* identification of a small-molecule activator of procaspase-3, first procaspase-activating compound (PAC-1; **1**, **Fig. 1a**). PAC-1 is powerfully proapoptotic in cancer cell lines in a manner proportional to procaspase-3 concentrations. Its proapoptotic effect is a result of its direct and immediate activation of procaspase-3, and it is effective against primary colon cancer isolates and in three different mouse models of cancer.

RESULTS

We screened approximately 20,500 structurally diverse small molecules for the ability to activate procaspase-3 *in vitro*. Procaspase-3 was expressed and purified in *Escherichia coli* according to standard procedures¹⁸. We added procaspase-3 to the wells of a 384-well plate and then added the compounds to a final concentration of approximately 40 μ M (the final concentration of procaspase-3 was 50 ng ml⁻¹). We incubated each plate for 2 h at 37 °C, and then we added the caspase-3 peptidic substrate acetyl Asp-Glu-Val-Asp-*p*-nitroanilide (Ac-DEVD-*p*Na) to a concentration of 200 μ M and followed the formation of the *p*-nitroaniline chromophore at 405 nm over the course of 2 h. Of the ~20,500 compounds evaluated, four induced a substantial increase over background in the hydrolysis of the peptidic caspase-3 substrate. Of those four, one showed a strong dose-dependent effect on *in vitro* procaspase-3 activation. This compound, PAC-1, gives half-maximal

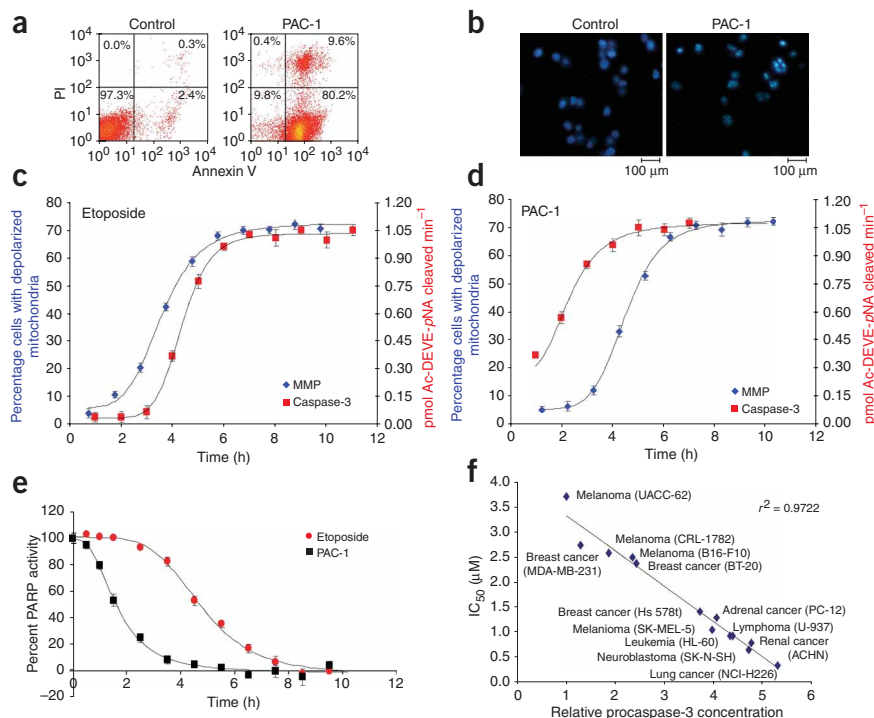
activation of procaspase-3 at a concentration of 0.22 μ M (**Fig. 1b**). PAC-1 was not simply increasing the activity of caspase-3 itself, as it had no effect on the catalytic activity of the fully processed caspase-3 enzyme (**Fig. 1b**). Control experiments indicated that PAC-1 has no effect on background hydrolysis of Ac-DEVD-*p*Na.

Procaspase-3 consists of a N-terminal prodomain (residues 1–28) followed by a large subunit (17 kDa) and a small subunit (12 kDa) that are separated by an intersubunit linker²⁵. *In vivo*, two procaspase-3 monomers assemble to form a homodimer that can be activated by cleavage at Asp175 in the intersubunit linker. The precise role of the prodomain is unclear, and cleavage in the intersubunit region alone is sufficient for full catalytic activity²⁶. Although procaspase-3 has enough catalytic activity to drive its own proteolytic maturation, it is highly resistant to this autoactivation because of the presence of the three-amino-acid safety catch¹⁸. However, when the safety catch is mutated, substantial autoactivation of procaspase-3 is observed¹⁸. It is possible that a small molecule containing substituents that are positively charged at physiological pH (such as the piperazine nitrogens in PAC-1) may directly interact with the tripartite acid safety catch, thereby inducing the autoactivation of procaspase-3. To directly assess the ability of PAC-1 to catalyze the maturation of procaspase-3 to the active caspase-3, we incubated the procaspase-3 protein with 100 μ M of PAC-1 for time points ranging from 1 to 5 h. As shown by western blotting, PAC-1 induced the cleavage of procaspase-3 in a time-dependent fashion (**Fig. 1c**), with >50% processing observed after 4 h as determined by densitometry. In contrast, procaspase-3 incubated in buffer showed virtually no autoactivation over the same time span. PAC-1 was also effective in this assay at a concentration of 5 μ M (**Supplementary Fig. 1** online).

We then made alanine substitutions in the key aspartic acid triad in the safety-catch region of procaspase-3 (residues Asp179, Asp180 and Asp181). Mutations at all of these positions decreased the ability of PAC-1 to activate procaspase-3 and increased the automaturation of procaspase-3, but certain mutations were more detrimental than

Figure 2 PAC-1 induces apoptosis in HL-60 cells.

(a) Phosphatidylserine exposure (as measured by annexin V staining and propidium iodide (PI) counterstaining) after a 20 h treatment with 100 μ M PAC-1. PAC-1 is also effective at 5 μ M in this assay (**Supplementary Fig. 2**). (b) Chromatin condensation as visualized by Hoechst-33258 staining after a 20-h treatment with 100 μ M PAC-1. (c) Mitochondrial membrane depolarization (MMP) and caspase-3-like activity in HL-60 cells treated with 10 μ M etoposide. (d) MMP and caspase-3-like activity in HL-60 cells treated with 100 μ M PAC-1. (e) PAC-1 treatment (100 μ M) induces a rapid decrease in cellular PARP activity in HL-60 cells, consistent with an immediate activation of cellular caspase-3 and caspase-7. In contrast, etoposide (10 μ M)-treated cells show a decrease in PARP activity at much later time points. (f) PAC-1 induces cell death in a procaspase-3-dependant manner. For several diverse cancerous cell lines, procaspase-3 concentrations were determined (by flow cytometry with an antibody to procaspase-3), and the IC_{50} of PAC-1 was measured (through a 72-h treatment with a range of PAC-1 concentrations and quantification using the MTS assay). PAC-1 is quite potent (IC_{50} = 0.35 μ M) in the NCI-H226 lung cancer cell line, which is known to have high concentrations of procaspase-3. All error bars are s.d.



others to activation of procaspase-3 by PAC-1 (**Fig. 1d**). Like caspase-3, caspase-7 exists as an inactive zymogen that is activated by proteolysis. Caspase-3 and caspase-7 are both executioner caspases and have considerable structural homology²⁷. Procaspase-7 is also predicted to have a safety-catch region similar to that of procaspase-3, although it has only two aspartic acids in the key triad (Asp-Thr-Asp) instead of three¹⁸. We found that PAC-1 can also activate procaspase-7, though it does so in a less efficient manner than for procaspase-3 (**Fig. 1e**; EC_{50} of 4.5 μ M versus 0.22 μ M for activation of procaspase-3). PAC-1 activated procaspase-7 and the Asp-Ala-Asp mutant of procaspase-3 with a similar potency (EC_{50} of 4.5 μ M versus EC_{50} of 2.77 μ M for the Asp-Ala-Asp procaspase-3 mutant). As expected, the effect of PAC-1 was abolished at low pH values, at which procaspase-3 undergoes rapid autoactivation (**Fig. 1f**).

We found PAC-1 to induce apoptosis in a variety of cancer cell lines. In HL-60 cells, the addition of PAC-1 leads to the appearance of many apoptotic hallmarks. During apoptosis, cells lose the ability to regulate the distribution of phospholipids in their cellular membrane, and phosphatidylserine is exposed on the outer membrane of apoptotic cells. PAC-1 treatment caused considerable phosphatidylserine exposure on the outer leaflet of the cell membrane as assessed by annexin V binding; this effect was observed at PAC-1 concentrations of 100 μ M (**Fig. 2a**) and 5 μ M (**Supplementary Fig. 2** online). Another apoptotic hallmark is the condensation of chromatin, which is due at least in part to the caspase-mediated activation of a DNase. This chromatin condensation was readily apparent in Hoechst-33258-stained HL-60 cells treated with PAC-1 (**Fig. 2b**). In addition, PAC-1 induced cleavage of the caspase substrate poly-ADP-ribose polymerase 1 (PARP-1; as assessed by an *in vivo* PARP activity assay²⁸) and caused mitochondrial membrane depolarization (see below). We also observed substantial cellular blebbing of cells treated with PAC-1 by microscopy. Furthermore, the toxicity of PAC-1 could be abolished in the presence of the caspase inhibitor Z-VAD-FMK (**Supplementary Fig. 3** online).

If PAC-1 induces apoptosis through direct activation of procaspase-3, then the time course of apoptotic events should be altered relative to that observed with standard proapoptotic agents. Etoposide is known to induce apoptosis through the intrinsic pathway; thus, mitochondrial membrane depolarization is followed by activation of procaspase-3 in etoposide-treated cells. Indeed, in HL-60 cells treated with 10 μ M etoposide, we observed mitochondrial membrane depolarization and then detected caspase-3-like activity (**Fig. 2c**). In contrast, treatment of cells with PAC-1 gave a markedly different result. With this compound, the first observed biochemical hallmark of apoptosis was caspase-3-like enzymatic activity. This activity was noted within minutes of PAC-1 addition, and over 50% activation takes place in just over 2 h, which is well before any substantial mitochondrial membrane depolarization (**Fig. 2d**). In the typical sequence of apoptotic events, the mitochondrial membrane depolarizes, caspases are activated and caspase substrates (such as the enzyme PARP-1) are cleaved. PARP-1 activity was rapidly reduced in cells treated with PAC-1, whereas this reduction was observed at later time points in etoposide-treated cells (**Fig. 2e**); control experiments showed that PAC-1 does not directly inhibit enzymatic activity of PARP-1 (**Supplementary Fig. 4** online). The observation that cells treated with PAC-1 show immediate caspase-3-like activity (before mitochondrial membrane depolarization) and a rapid cleavage of a caspase substrate (PARP-1) indicates that PAC-1 exerts its cellular toxicity through the direct activation of procaspase-3.

To further define the potency of PAC-1, we assessed the compound's ability to induce cell death in cancer cell lines with varying concentrations of procaspase-3. We first determined the concentrations of procaspase-3 present in several cancer cell lines (leukemia, lymphoma, melanoma, neuroblastoma, breast cancer, lung cancer, adrenal cancer and renal cancer). We obtained the IC_{50} values for cell death induction for PAC-1 versus these cell lines. The combined data shows a strong correlation between cellular concentration of

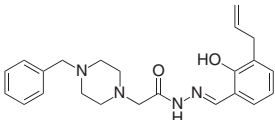
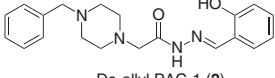
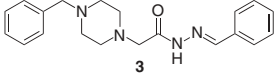
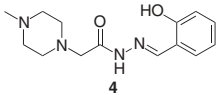
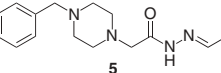
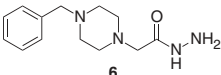
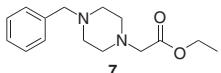
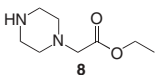
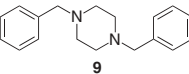
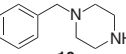
Compound	EC ₅₀ (μM) for procaspase-3 activation	IC ₅₀ (μM) for death induction in HL-60 cells
 PAC-1 (1)	0.22	0.92
 De-allyl PAC-1 (2)	0.43	1.74
 3	>50	>100
 4	>50	>100
 5	>50	>100
 6	>50	>100
 7	>50	>100
 8	>50	>100
 9	>50	>100
 10	>50	>100

Figure 3 PAC-1 and de-allyl PAC-1 activate procaspase-3 *in vitro* and induce death in cancer cells in cell culture, but other structural analogs have no procaspase-3-activating effect *in vitro* and do not induce death in cell culture.

pro-caspase-3 and sensitivity to PAC-1 (Fig. 2f). PAC-1 is most potent against the lung cancer cell line NCI-H226, with an IC₅₀ of 0.35 μM. In accordance with previous findings²⁴, we found this cell line to have a concentration of procaspase-3 that is five times that of baseline levels. Notably, there is one cancer cell line (MCF-7, breast cancer cells) that has no expression of procaspase-3. PAC-1 had virtually no effect on MCF-7 cells: it induced death with an IC₅₀ > 75 μM.

In contrast, etoposide showed no such correlation between potency in cell culture and cellular concentrations of procaspase-3 (Supplementary Fig. 5 online). For instance, etoposide was ineffective (IC₅₀ > 50 μM) in inducing death in three of the melanoma cell lines (UACC-62, CRL-1782 and B16-F10), the breast cancer cell line (Hs 578t) and the lung cancer cell line (NCI-H226); these cell lines have relative procaspase-3 concentrations of 1.0, 2.4, 1.9, 3.7 and 5.3, respectively. Etoposide was effective (IC₅₀ < 1 μM) versus HL-60, U-937, SK-N-SH and PC-12, which have relative procaspase-3 concentrations of 4.3, 4.0, 4.7 and 4.4, respectively. Thus, overall there

is no correlation between procaspase-3 concentrations and IC₅₀ for etoposide.

We synthesized and evaluated several derivatives of PAC-1 for both their procaspase-3-activating properties and their effects on cancer cells in cell culture (Fig. 3). The PAC-1 derivative that lacks the allyl group, de-allyl PAC-1 (2), was able to induce activation of procaspase-3 and cell death at levels similar to those induced by PAC-1. However, all other derivatives created (3–10) showed no activity in either assay. Thus, whereas it seems the allyl group is dispensable for biological activity, the phenolic hydroxyl and benzyl moieties are both critical for PAC-1 activity. These data are also consistent with the proposed mechanism of action of PAC-1; compounds that do not activate procaspase-3 *in vitro* have no proapoptotic effect on cancer cells in culture.

To test this direct, small molecule-mediated procaspase-3 activation strategy in clinical isolates of cancer, we obtained freshly resected colon tumors (together with adjacent noncancerous tissue) from 23 people at Carle Foundation Hospital (Urbana, Illinois, USA). We separated the cancerous and noncancerous tissue and evaluated the cells derived from these for their concentrations of procaspase-3 and their sensitivity to PAC-1 (Supplementary Fig. 6 online). In all cases the cancerous cells had elevated concentrations (1.7-fold to 19.7-fold, with an average of 8.4-fold) of procaspase-3 relative to cells from the adjacent noncancerous tissue from the same person (Fig. 4a). Further, these cancerous cells were quite susceptible to death induction by PAC-1. PAC-1 induced cell death in the primary cancerous cells with IC₅₀ values from 0.003 to 1.41 μM, whereas it induced cell death in the adjacent noncancerous tissue with IC₅₀ values from 5.02 to 9.98 μM (Fig. 4b and Table 1). The cells from cancerous tissue that had elevated concentrations of procaspase-3 were extremely sensitive to PAC-1 (Fig. 4b). For example, as a single-entity agent PAC-1 induced death in the cancer cells from subject 21 with an IC₅₀ of 3 nM, and these cells were over 2,000-fold more sensitive to PAC-1 than cells from the adjacent normal tissue (Table 1).

In addition to evaluating PAC-1 against cells from the noncancerous tissue of the 23 individuals, we also evaluated PAC-1 against four other noncancerous cell types: white blood cells isolated from the bone marrow of a healthy donor, Hs888Lu (lung fibroblast cells), MCF-10A (breast fibroblast cells) and Hs578Bst (breast epithelial cells). Notably, the noncancerous cell types are among those with the least procaspase-3, and PAC-1 is comparatively less able to induce death in these cells, with IC₅₀ values of 3.2–8.5 μM (Fig. 4b). Thus PAC-1 induces death in a wide variety of cell types (noncancerous cell lines, noncancerous primary cells, cancerous cell lines and primary cancerous cells) in a manner directly related to the concentration of procaspase-3. The elevation of procaspase-3 concentrations in cancerous cells allows PAC-1 to selectively induce death in these cell types.

We evaluated PAC-1 in a mouse xenograft model using a slow-release mode of drug delivery. In this model, subcutaneous tumors were formed in ovariectomized female athymic BALB/c (nude, *nu/nu*) mice using the ACHN (renal cancer) cell line. Once the tumors were larger than ~30 mm² in area, we administered the drug via implantation of a pellet of PAC-1 and cholesterol, providing for slow and steady levels of compound release. We used three groups of mice, with pellets containing 0 mg, 1 mg and 5 mg of PAC-1 (six mice per group, four tumors per mouse). Tumor growth was significantly retarded in the mice that were implanted with the pellet containing 5 mg of PAC-1 (*p* < 0.005; Fig. 5a). Evaluation of food intake in the last week of the experiment showed no difference in food consumption among the three groups of mice. After the mice were killed, plasma samples were taken from each mouse, and the PAC-1 content of each sample was

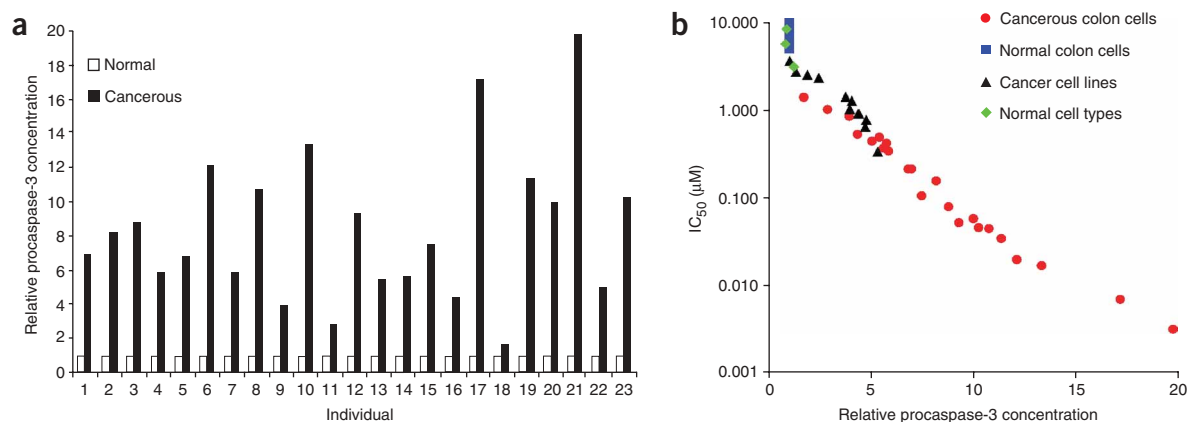


Figure 4 PAC-1 induces death in cells isolated from freshly resected colon tumors. **(a)** Procaspase-3 concentrations are elevated in cells derived from freshly resected colon cancer tissue. Freshly resected primary colon tumors (together with adjacent noncancerous tissue) were obtained from 23 people, the cancerous and noncancerous tissue were separated, and the procaspase-3 concentrations were measured for each using an antibody to procaspase-3 and flow cytometry. On average, cells from the cancerous tissue had an 8.4-fold elevation in procaspase-3 relative to cells derived from the adjacent noncancerous tissue from the same person. **(b)** PAC-1 induces cell death in a manner proportional to the cellular concentration of procaspase-3. The red circles represent the primary cancerous cells from the 23 colon tumors. The black triangles represent the same cancer cell lines depicted in **Figure 2f**. The green diamonds are four noncancerous cell types: Hs888Lu (lung fibroblast cells), MCF-10A (breast fibroblast cells), Hs578Bst (breast epithelial cells) and white blood cells isolated from the bone marrow of a healthy donor. The blue squares are the primary noncancerous cells isolated from the tumor margins of the 23 people.

analyzed. For mice that received a 5-mg pellet of PAC-1, PAC-1 was present at a concentration of $4.4 \text{ nM} \pm 1.1$ in the plasma after the 54-d experiment (**Supplementary Fig. 7** online). This relatively low serum concentration of PAC-1 suggests that administration of a larger dose could lead to actual tumor regression, instead of the tumor growth retardation we observed.

We evaluated PAC-1 in a second mouse xenograft model in which we used oral administration as the drug delivery mode. In this model, subcutaneous xenograft tumors were formed in male athymic BALB/c nude mice (5 weeks old, SLC) using the NCI-H226 (lung cancer) cell line (eight mice per group, three tumors per mouse). After tumors were formed, we treated the mice with PAC-1 via oral gavage once a day for 21 d at concentrations of 0, 50 and 100 mg kg^{-1} and killed the mice 1 week later. We observed no differences in body weight among the three groups of mice, and there was no evidence of gross toxicity. The data indicate that oral administration of PAC-1 significantly retards tumor growth in a dose-dependent manner ($P < 0.001$; **Fig. 5b**).

To determine whether tumor cells were dying through apoptosis, we subjected tumors removed at the end of this experiment to terminal dUTP nick-end labeling (TUNEL) analysis. This common apoptotic assay assesses the number of 3' hydroxyl ends present in DNA when it is fragmented during apoptosis. The number of TUNEL-positive cells increased with the dose of PAC-1 (**Fig. 5c**), a result consistent with the notion that PAC-1 induces apoptosis *in vivo*. In addition, analysis of tumor cells by western blotting showed that procaspase-3 is processed in the tumors from mice treated with PAC-1 (**Fig. 5d**).

Finally, we evaluated PAC-1 in a mouse model in which we injected NCI-H226 cells into male athymic *BALB/c*^{-/-} mice via the tail vein. The total experiment lasted 28 d. We treated one group of mice once a day with PAC-1 (100 mg kg^{-1}) via oral gavage on days 1–4 and 7–11; on the other days these mice did not receive PAC-1 or vehicle. A second group of mice received only vehicle on days 1–4 and 7–11. We observed no differences in body weight between the two groups of mice, and there was no evidence of gross toxicity. After 28 d the mice were killed and their lungs examined. NCI-H226 lung cancer cells

were able to infiltrate the lung tissue and form tumors (**Fig. 5e**). The exposed lung of control mice showed very large gray tumors covering almost half of the outer lung surface, whereas the lungs of mice treated with PAC-1 showed only very small gray tumors. The lungs from the mice in this experiment were then sectioned, stained and imaged. In the control mice the gray NCI-H226 cells almost completely overtook

Table 1 IC₅₀ values of PAC-1 versus cells isolated from primary cancerous and noncancerous colon tissue

Individual	PAC-1 IC ₅₀ (µM)	
	Normal	Cancerous
1	6.78	0.212
2	9.79	0.154
3	6.61	0.080
4	9.50	0.340
5	6.88	0.216
6	6.28	0.020
7	7.34	0.422
8	5.67	0.045
9	6.54	0.844
10	9.98	0.017
11	5.94	1.030
12	5.63	0.052
13	5.50	0.499
14	7.58	0.366
15	5.96	0.106
16	5.02	0.527
17	5.17	0.007
18	6.39	1.410
19	5.41	0.034
20	6.84	0.058
21	6.25	0.003
22	5.73	0.439
23	5.28	0.046

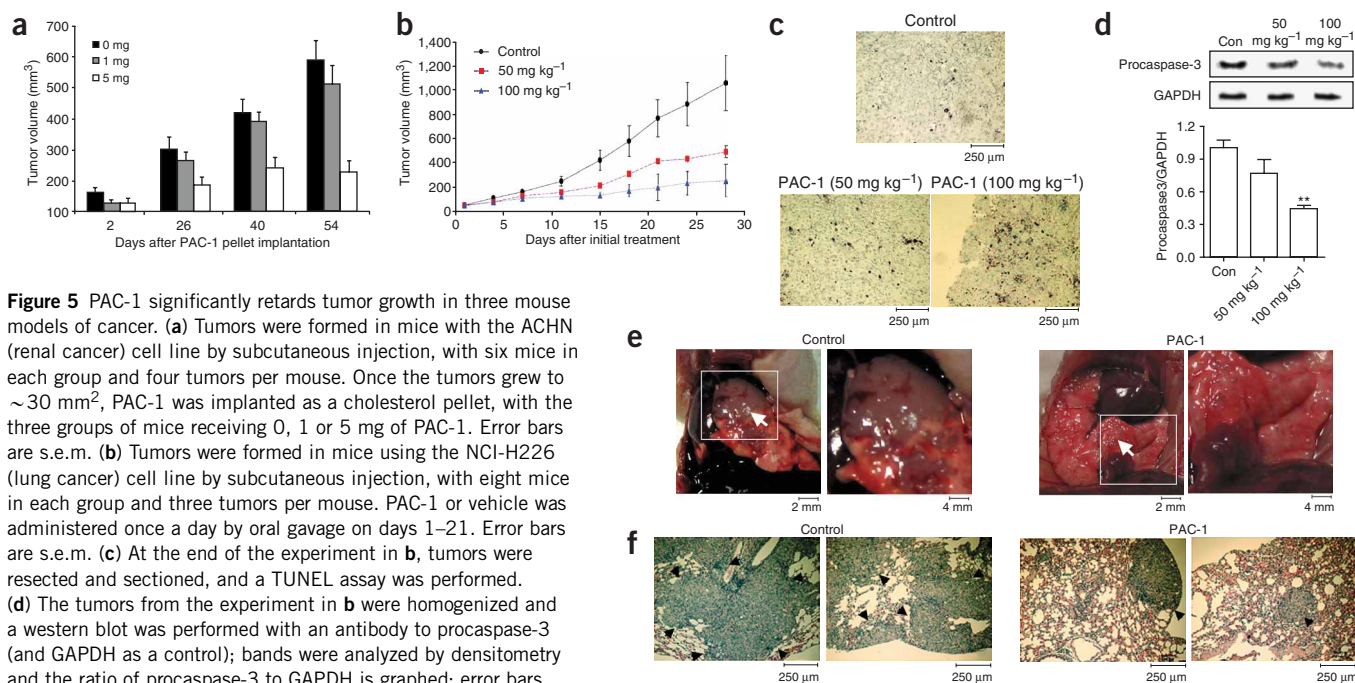


Figure 5 PAC-1 significantly retards tumor growth in three mouse models of cancer. **(a)** Tumors were formed in mice with the ACHN (renal cancer) cell line by subcutaneous injection, with six mice in each group and four tumors per mouse. Once the tumors grew to ~ 30 mm², PAC-1 was implanted as a cholesterol pellet, with the three groups of mice receiving 0, 1 or 5 mg of PAC-1. Error bars are s.e.m. **(b)** Tumors were formed in mice using the NCI-H226 (lung cancer) cell line by subcutaneous injection, with eight mice in each group and three tumors per mouse. PAC-1 or vehicle was administered once a day by oral gavage on days 1–21. Error bars are s.e.m. **(c)** At the end of the experiment in **b**, tumors were resected and sectioned, and a TUNEL assay was performed. **(d)** The tumors from the experiment in **b** were homogenized and a western blot was performed with an antibody to procaspase-3 (and GAPDH as a control); bands were analyzed by densitometry and the ratio of procaspase-3 to GAPDH is graphed; error bars are s.d. ** indicates a statistical difference from the control; $P < 0.05$. **(e)** Mice were injected with the NCI-H226 cell line. The mice were treated with PAC-1 (100 mg kg⁻¹) via oral gavage following the protocol described in the text. The lungs of control mice have a large amount of gray tumor mass, whereas the mice that received PAC-1 have almost no visible tumor. **(f)** Resected lungs were sectioned, stained and imaged. Lungs from mice in the control group have multiple metastatic foci and a much larger tumor burden, whereas lungs from mice treated with PAC-1 show a greatly reduced tumor burden.

the normal pink lung tissue, whereas in the mice treated with PAC-1 we found only isolated tumors in the lungs (Fig. 5f).

DISCUSSION

Cancerous cells typically have a lower sensitivity than normal cells to proapoptotic signals owing to the mutation or aberrant expression of an assortment of proteins in the apoptotic cascade. As such, many types of cancer are notoriously resistant to not only the endogenous signals for apoptotic cell death but also to the chemotherapeutic agents that act through similar mechanisms. The paradoxical elevation of procaspase-3 concentrations in certain cancers provides an opportunity to use this existing intracellular pool of protein to directly induce apoptosis, thereby bypassing the often nonfunctional upstream portion of the cascade. PAC-1 induces the autoactivation of procaspase-3 *in vitro*; in cell culture, PAC-1 treatment induces rapid caspase-3-like activity. It is likely that the caspase-3-mediated cleavage of antiapoptotic proteins (such as Bcl-2 and Bcl-XL)^{29–31} then induces depolarization of the mitochondrial membrane and amplifies apoptosis. In addition, the potency of PAC-1 toward a variety of cancerous and noncancerous cell types is proportional to the concentration of procaspase-3 in the cell. As the primary cancerous cells isolated from resected colon tumors have elevated concentrations of procaspase-3, these cells are considerably more sensitive to PAC-1 than cells from adjacent noncancerous tissue. It is worth noting that several of the cell lines against which PAC-1 is effective have faulty apoptotic pathways that make them resistant to apoptosis; for instance, Apaf-1 expression in SK-MEL-5 cells is lower than that in normal cells⁵, and Bcl-2 is overexpressed in the NCI-H226 lung cancer cell line³². Finally, PAC-1 is effective in three different mouse models of cancer, including two in which PAC-1 is administered orally.

Our data here support the notion that procaspase-3-activating compounds can be effective against common cancers in which procaspase-3 concentrations are aberrantly high. Although cellular procaspase-3 quantities have not been fully defined for all cancer types, it is now clear that many cancers have elevated concentrations of procaspase-3 (refs. 18–23), and others have heightened or reduced concentrations of procaspase-3 depending on the cancer subtype^{33–35}. A systematic and thorough analysis of procaspase-3 concentrations in a variety of cancer types and subtypes is therefore needed to determine which cancers are most amenable to treatment with a procaspase-3 activator.

Assessment of procaspase-3 concentrations in cancer biopsies is simple and rapid, and the data presented herein indicate that cellular concentrations of procaspase-3 can be used to predict PAC-1 efficacy. As such, the potential effectiveness of a compound such as PAC-1 could be assessed *a priori* with a high degree of accuracy, and people with cancer could be preselected for treatment with a procaspase-3 activator based on the concentration of procaspase-3 in their tumor cells. Such personalized medicine strategies are preferential to therapies that rely on general cytotoxins, and these strategies are the future of anticancer therapy.

METHODS

Further detailed methods can be found in **Supplementary Methods** online.

Library screen. Procaspase-3 was incubated with approximately 20,500 compounds at a concentration of ~ 40 μ M for 2 h. Ac-DEVD-pNA was added and the plate was then read every 2 min at 405 nm for 2 h. The slope of the linear portion for each well was used to determine the activity of caspase-3.

Activation curves. Various concentrations of compound were added to procaspase-3, active caspase-3, procaspase-7 and active caspase-7 and incubated for 12 h at 37 °C. Ac-DEVD-pNA was added and the plate was read every 2 min at 405 nm for 2 h. The slope of the linear portion for each well was determined, and the relative increase in activation from untreated control wells was calculated.

PAC-1 activation gel. Procaspase-3 was incubated in the presence or absence of 100 μM PAC-1 for varying times at 37 °C. SDS-loading buffer was then added and the samples were run on a 12% SDS-PAGE gel. Proteins were transferred to nitrocellulose overnight. Blots were washed and then blocked with a 10% milk solution. Blots were then incubated in a 1:5,000 dilution of antibody against Penta His Alexa Fluor 647 (Qiagen) for 2 h, washed and scanned.

Safety-catch mutations. The Asp-Asp-Asp procaspase-3 safety catch was mutated to Ala-Asp-Asp, Asp-Ala-Asp and Asp-Asp-Ala. Various concentrations of PAC-1 were added to wild-type procaspase-3 and to the various mutant versions of procaspase-3 and incubated for 12 h at 37 °C. Ac-DEVD-pNA was then added to each well and the plate was read every 2 min at 405 nm for 2 h. The slope of the linear portion for each well was determined, and the relative increase in activity for each mutant was calculated.

Effect of pH on PAC-1 activation of procaspase-3. Procaspase-3 was incubated for 12 h at 37 °C in buffers of various pH values. Ac-DEVD-pNA was added, and the plate was read every 2 min at 405 nm for 2 h. The slope of the linear portion for each well was determined, and the relative increase in activation for each pH value was calculated.

Annexin V staining. PAC-1 in DMSO or DMSO alone was added to HL-60 cells and incubated at 37 °C. The cells were harvested by centrifugation and washed twice in PBS. The cells were then washed and resuspended in annexin V binding buffer. Annexin V-Alexa Fluor 488 conjugate (Molecular Probes) was added and incubated at room temperature (23 °C) for 15 min. Annexin V binding buffer was then added, followed by the addition of propidium iodide. The fluorescence intensity of each cell was determined by flow cytometry at 525 nm (green channel) and 675 nm (red channel). At least 50,000 cells were analyzed in each experiment.

Condensed-chromatin staining. PAC-1 in DMSO or DMSO alone was added to HL-60 cells and incubated for 20 h. The cells were harvested by centrifugation, washed in PBS and fixed by the addition of ice-cold (0 °C) 100% ethanol. The cells were incubated overnight at 4 °C. Fixed cells were incubated with Hoechst-33258 (Molecular Probes) for 30 min at room temperature. A drop of cells was added to a microscope slide. Condensed chromatin was observed at ×400 magnification.

In vivo determination of mitochondrial membrane potential. PAC-1 in DMSO or DMSO alone was added to HL-60 cells and incubated for various times. The cells were harvested by centrifugation and washed in PBS. JC-9 dye (Molecular Probes) was added and the cells were incubated at room temperature for 10 min. The cells were then washed in PBS and the fluorescence intensity of each cell was determined by flow cytometry at 525 nm (green channel) and 675 nm (red channel). 50,000 cells were analyzed in each experiment. The shift in the red channel was then used to determine the amount of mitochondrial membrane depolarization.

In vivo determination of caspase-3-like activity. A range of concentrations of PAC-1 was added to HL-60 cells and incubated for various times. The cells were washed with PBS, resuspended in ice-cold caspase assay buffer and lysed by sonication. Ac-DEVD-pNA was added and the plate was read every 2 min at 405 nm for 2 h. The slope of the linear portion for each well was determined and the amount of Ac-DEVD-pNA cleaved per minute was calculated.

In vivo determination of PARP cleavage. NAD⁺ alone or NAD⁺ with PAC-1 was added to HL-60 cells and incubated for various times. Lysing PARP buffer containing 25 mM H₂O₂ was added and the cells were incubated for 60 min at 37 °C. To determine the amount of NAD⁺ still present, KOH and acetophenone were added followed by a 10 min incubation at 4 °C. 88% (v/v) formic acid was added followed by a 5-min incubation in an oven set to 110 °C. The

fluorescence was determined and the number of moles of NAD⁺ cleaved per minute was then calculated. The remaining PARP activity as compared to control wells was determined.

Isolation of normal and cancerous colon cells. Cancerous colon tissue with attached normal tissue was resected from volunteers at Carle Foundation Hospital (Urbana, Illinois, USA) collected under a protocol approved by the hospital's Institutional Review Board (#04-63). The tissue was transported immediately to the laboratory in ice-cold PBS. The normal tissue was removed from the cancerous tissue using a scalpel and both tissues were then coarsely minced. The minced tissue was digested with dispase I and collagenase IV for 90 min at 37 °C. The freed cells were washed and resuspended in RPMI-1640 containing 10% FBS.

Relative concentration of procaspase-3 in various cell lines. Cells were washed in PBS, resuspended in ice-cold 100% ethanol and fixed overnight at 4 °C. The cells were then washed with PBS and incubated with an antibody to caspase-3 (Sigma) for 2 h at room temperature. The cells were then washed in PBS and incubated with an anti-mouse Cy3-labeled antibody for 2 h at room temperature. The cells were washed with PBS and the fluorescence intensity of each cell was determined by flow cytometry at 675 nm (red channel). At least 20,000 cells were analyzed in each experiment. The median of the population was used to determine the relative concentration of procaspase-3 in each cell line.

Determination of IC₅₀ values in various cell lines. Various concentrations of etoposide or PAC-1 were added to cells and incubated for 24 h and 72 h for etoposide and PAC-1, respectively. Cell death was quantified by the addition of MTS/PMS CellTiter 96 Cell Proliferation Assay reagent (Promega). The plates were incubated at 37 °C for approximately 1 h (until the colored product formed), and the absorbance was measured at 490 nm.

Inhibition of ACHN xenograft growth by subcutaneous PAC-1 release. Ovariectomized female athymic BALB/c mice 35 d of age were used for the following experiment. Animal research was performed in accordance with a protocol approved by the University of Illinois at Urbana-Champaign Institutional Animal Care and Use Committee.

Various ratios of PAC-1 and cholesterol were mixed and pelleted into a 3-mm-diameter 20-mg (total weight) pellet. Pellets contained either 0 mg, 1 mg or 5 mg PAC-1.

ACHN cancer cells were resuspended in Matrigel (BD Biosciences) and injected subcutaneously into the four flanks of the back of each animal.

Tumor growth and body weight were measured weekly, and tumor volume was calculated using the formula $v = 0.5 \times a \times b^2$, where a and b are the largest and smallest tumor diameters, respectively. After 4 weeks, mice were randomly divided into four treatment groups (six mice per group, average tumor surface area 34.3 mm²) and PAC-1 plus cholesterol or control (cholesterol only) pellets were implanted subcutaneously. At the end of the study (8 weeks after pellet implantation), food intake was measured for two consecutive 24-h periods and tumors and blood samples were collected.

Plasma samples were obtained from killed mice on completion of the xenograft study. A deuterated version of PAC-1 containing seven deuterium atoms was synthesized as an internal standard. A standard curve was generated using PAC-1 in the concentration range of 0.25–25 fmol μl⁻¹ ($R^2 = 0.9997$). Deuterated PAC-1 was added to each serum sample to yield a final concentration of 1 fmol μl⁻¹. The samples were analyzed by LC/MS/MS, and the limit of detection was 0.15 fmol μl⁻¹, the intraday and interassay precision ranged between 2% and 17% relative s.d. and the accuracies ranged between 102% and 134%. The average internal standard recovery was determined to be 61%. Using the recovery value, the concentration of PAC-1 in each plasma sample was calculated.

Inhibition of NCI-H226 xenograft growth by PAC-1 as administered by oral gavage. To generate tumors, 100 μl of a single-cell suspension containing 2×10^6 NCI-H226 cells were injected subcutaneously into the flanks of athymic nude mice. Tumor volume was calculated using the mean diameter measured with vernier calipers using the formula $v = 0.5 \times a \times b^2$, where a and b are the smallest and largest tumor diameters, respectively. PAC-1

treatment was administered after the tumors reached a size of approximately 50 mm³ (approximately 4 weeks after implantation). The vehicle control and PAC-1 were administered at 50 and 100 mg kg⁻¹ via oral gavage (in a mixture of 24:1 vegetable oil/DMSO) once a day for 21 d. Tumor volume was measured twice weekly for 4 weeks. Tumors were collected, homogenized and normalized to the total amount of protein. The samples were then run on an SDS-PAGE gel and transferred to nitrocellulose. The blot was stained with antibodies specific for procaspase-3 and GAPDH as a control. The full-length procaspase-3 bands were further analyzed by densitometry and plotted as a ratio of procaspase-3 per GAPDH.

Inhibition of intravenously administered NCI-H226 tumor growth by PAC-1 as administered by oral gavage. To generate tumors, 100 µl of a single-cell suspension containing 2 × 10⁶ NCI-H226 cells were injected intravenously into the tail vein of athymic nude mice. PAC-1 or vehicle (four mice per group) was administered via oral gavage (in a mixture of 24:1 vegetable oil/DMSO) at 100 mg kg⁻¹ once a day on days 0–4 and days 7–11. The mice were killed after 28 d and the thoracic cavity was exposed. Photographs of tumor load in the lung tissue were taken. Lungs were then sectioned, stained and photographed.

Note: Supplementary information is available on the Nature Chemical Biology website.

ACKNOWLEDGMENTS

This work was supported by the National Science Foundation (NSF CAREER award to P.J.H., CHE-0134779), the University of Illinois (to P.J.H.) and the National Institutes of Health (Grant CA77355 to W.G.H. and AG024387 to W.G.H. and D.R.D.). K.S.P. is supported by a fellowship from the American Chemical Society Division of Medicinal Chemistry. M.S.H. was supported by National Institute of Environmental Health Sciences Training Grant 5T32ES007326-05. J.T.K., S.K.H. and H.J. are recipients of a Brain Korea 21 fellowship. M.H.C. is supported by a Korea Science and Engineering Foundations (KOSEF), Ministry of Science and Technology (MOST) grant (550-20060062). We thank P. Tender and L. Tangen (Carle Foundation Hospital) for the primary colon cancer samples. We thank R. Hoffman (University of Illinois-Chicago Cancer Center) for the generous gift of human bone marrow. We thank G. Salvesen (Burnham Institute) for the gift of the procaspase-3 and procaspase-7 expression vectors. We thank D. Goode and A. Sharma (University of Illinois) for synthesis of the peptidic caspase substrate. We acknowledge the assistance of the Flow Cytometry Facility of the Biotechnology Center at the University of Illinois.

AUTHOR CONTRIBUTIONS

K.S.P. and P.J.H. were responsible for designing the experiments and writing the manuscript. K.S.P. conducted the high-throughput screen, all *in vitro* and all cell culture experiments with PAC-1, and all experiments with the primary colon tumors. G.W.C. and J.M.P. assisted with the high-throughput screen. J.S.S. was responsible for the synthesis of PAC-1 and its derivatives. M.S.H. and W.G.H. evaluated PAC-1 in the ACHN xenograft model. J.T.K., S.K.H., H.J. and M.H.C. evaluated PAC-1 in the NCI-H226 xenograft models. D.R.D. and M.I.C. determined the concentrations of PAC-1 in mouse serum.

COMPETING INTERESTS STATEMENT

The authors declare that they have no competing financial interests.

Published online at <http://www.nature.com/naturechemicalbiology>
Reprints and permissions information is available online at <http://npg.nature.com/reprintsandpermissions/>

- Hanahan, D. & Weinberg, R.A. The hallmarks of cancer. *Cell* **100**, 57–70 (2000).
- Lowe, S.W., Cepero, E. & Evan, G. Intrinsic tumor suppression. *Nature* **432**, 307–315 (2004).
- Vogelstein, B. & Kinzler, K.W. Achilles' heel of cancer. *Nature* **412**, 865–866 (2001).
- Traven, A., Huang, D.C. & Lithgow, T. Protein hijacking: key proteins held captive against their will. *Cancer Cell* **5**, 107–108 (2004).

- Soengas, M.S. *et al.* Inactivation of the apoptosis effector Apaf-1 in malignant melanoma. *Nature* **409**, 207–211 (2001).
- Wajant, H. Targeting the FLICE inhibitory protein (FLIP) in cancer therapy. *Mol. Interv.* **3**, 124–127 (2003).
- Okada, H. & Mak, T.W. Pathways of apoptotic and non-apoptotic death in tumour cells. *Nat. Rev. Cancer* **4**, 592–603 (2004).
- Denicourt, C. & Dowdy, S.F. Targeting apoptotic pathways in cancer cells. *Science* **305**, 1411–1413 (2004).
- Green, D.R. & Kroemer, G. Pharmacological manipulation of cell death: clinical applications in sight? *J. Clin. Invest.* **115**, 2610–2617 (2005).
- Vassilev, L.T. *et al.* *In vivo* activation of the p53 pathway by small-molecule antagonists of MDM2. *Science* **303**, 844–848 (2004).
- Degterev, A. *et al.* Identification of small-molecule inhibitors of interaction between the BH3 domain and Bcl-XL. *Nat. Cell Biol.* **3**, 173–182 (2001).
- Becattini, B. *et al.* Rational design and real time, in-cell detection of the proapoptotic activity of a novel compound targeting Bcl-XL. *Chem. Biol.* **11**, 389–395 (2004).
- Wang, J.-L. *et al.* Structure-based discovery of an organic compound that binds Bcl-2 protein and induces apoptosis of tumor cells. *Proc. Natl. Acad. Sci. USA* **97**, 7124–7129 (2000).
- Li, L. *et al.* A small molecule Smac mimic potentiates TRAIL- and TNF α -mediated cell death. *Science* **305**, 1471–1474 (2004).
- Nguyen, J.T. & Wells, J.A. Direct activation of the apoptosis machinery as a mechanism to target cancer cells. *Proc. Natl. Acad. Sci. USA* **100**, 7533–7538 (2003).
- Jiang, X. *et al.* Distinctive roles of PHAP proteins and prothymosin- α in a death regulatory pathway. *Science* **299**, 223–226 (2003).
- Boatright, K.M. & Salvesen, G.S. Mechanisms of caspase activation. *Curr. Opin. Cell Biol.* **15**, 725–731 (2003).
- Roy, S. *et al.* Maintenance of caspase-3 proenzyme dormancy by an intrinsic "safety catch" regulatory tripeptide. *Proc. Natl. Acad. Sci. USA* **98**, 6132–6137 (2001).
- Nakagawara, A. *et al.* High levels of expression and nuclear localization of interleukin-1 β converting enzyme (ICE) and CPP32 in favorable human neuroblastomas. *Cancer Res.* **57**, 4578–4584 (1997).
- Izban, K.F. *et al.* Characterization of the interleukin-1 β -converting enzyme/Ced-3-family protease, caspase-3/ CPP32, in Hodgkin's disease. *Am. J. Pathol.* **154**, 1439–1447 (1999).
- Estrov, Z. *et al.* Caspase 2 and caspase 3 protein levels as predictors of survival in acute myelogenous leukemia. *Blood* **92**, 3090–3097 (1998).
- Fink, D. *et al.* Elevated procaspase levels in human melanoma. *Melanoma Res.* **11**, 385–393 (2001).
- Persad, R. *et al.* Overexpression of caspase-3 in hepatocellular carcinomas. *Mod. Pathol.* **17**, 861–867 (2004).
- Svingen, P.A. *et al.* Components of the cell death machine and drug sensitivity of the National Cancer Institute Cell Line Panel. *Clin. Cancer Res.* **10**, 6807–6820 (2004).
- Pop, C., Feeney, B., Tripathy, A. & Clark, A.C. Mutations in the procaspase-3 dimer interface affect the activity of the zymogen. *Biochemistry* **42**, 12311–12320 (2003).
- Stennicke, H.R. *et al.* Pro-caspase-3 is a major physiologic target of caspase-8. *J. Biol. Chem.* **273**, 27084–27090 (1998).
- Denault, J.-B. & Salvesen, G.S. Human caspase-7 activity and regulation by its N-terminal peptide. *J. Biol. Chem.* **278**, 34042–34050 (2003).
- Putt, K.S., Beilman, G.J. & Hergenrother, P.J. Direct quantitation of poly(ADP-ribose) polymerase (PARP) activity as a means to distinguish necrotic and apoptotic death in cell and tissue samples. *ChemBioChem* **6**, 53–55 (2005).
- Liang, Y., Nylander, K.D., Yan, C. & Schor, N.F. Role of caspase 3-dependent Bcl-2 cleavage in potentiation of apoptosis by Bcl-2. *Mol. Pharmacol.* **61**, 142–149 (2002).
- Fujita, N., Nagahashi, A., Nagashima, K., Rokudai, S. & Tsuruo, T. Acceleration of apoptotic cell death after the cleavage of Bcl-XL protein by caspase-3-like proteases. *Oncogene* **17**, 1295–1304 (1998).
- Earnshaw, W.C., Martins, L.M. & Kaufmann, S.H. Mammalian caspases; structure, activation, substrates, and functions during apoptosis. *Annu. Rev. Biochem.* **68**, 383–424 (1999).
- Koty, P.P., Zhang, H. & Levitt, M.L. Antisense bcl-2 treatment increases programmed cell death in non-small cell lung cancer cell lines. *Lung Cancer* **23**, 115–127 (1999).
- O'Donovan, N. *et al.* Caspase 3 in breast cancer. *Clin. Cancer Res.* **9**, 738–742 (2003).
- Vakkala, M., Paakko, P. & Soini, Y. Expression of caspases 3, 6 and 8 is increased in parallel with apoptosis and histological aggressiveness of the breast lesion. *Br. J. Cancer* **81**, 592–599 (1999).
- Devarajan, E. *et al.* Down-regulation of caspase 3 in breast cancer: a possible mechanism for chemoresistance. *Oncogene* **21**, 8843–8851 (2002).

